Structural basis of nucleotide exchange and client binding by the novel Hsp70-cochaperone Bag2

Zhen Xu, Richard C Page, Michelle M Gomes, Ekta Kohli, Jay C Nix, Andrew B Herr, Cam Patterson, and Saurav Misra.

Supplementary Materials (5 Figures, 1 Table, Methods, References)

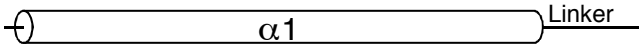


```
dimer                    dd dd  dd  dd dd  dd  d  dd  d
Hsc70                    h                              hhhhh hhhh
peptide                 11
Mm    91 TLTVEVSVETIRNPQQEESLKHATRIIDEVVSKFLDDLGNAKSHLMSLYSACSSEVPPGP 150
Hs    91 TLTVEVSVETIRNPQQQESLKHATRIIDEVVNKFLDDLGNAKSHLMSLYSACSSEVPHGP 150
Bt    91 TLTVEVSVETIRSPQQQESLKHATRIIDEVVSKFLDDLGNARSHLMSLYSACSSEVPAGP 150
Md    91 TLTVEVSVETIRNPQQQESLRHATMIIDEVVNKFLDDLENAKSHLMSLYGACSSEVPPGP 150
Oa    91 TLTVEVSVETIRNPQQQESLRNATLIIDEVVNKFLDDLENAKSHLMSLYGACTSEVPPGP 150
Gg   108 TLTVEVSVETIRNAQQQESLLHATRMIDEIVNKLLDDLEDAKIRLMSLYGACTSDVPAGP 167
Xt    96 TLTVAVAVETIRNPQQESSLQQASMIIDEILKKVMDNLENGRKQLMGLYGACSSEVPAGP 155
Br    94 TLTVKVSLETIRNQQQEEALQKAMKMIDEITEKLLEDLQSARTRLEALHAACVSDAPPVP 153
Ce   352 TKTVQVVVETPRNEEQKKALEDATLMIDEVGEMMHSNIEKAKLCLQTYMNACSYEETAGA 411
Spu  106 CLTVDINIQTIRTPAQEESLRKVKGYLRDLIDTMQANLEQSSRRVKLYLNSCLG[4]MGP 166
Dm   154 LATVELRVRTVRDNSQEDSLSQINVLIDSMIKMGDPVIGRQRCQFYLNACCSSS[15]GP 224
Am    87 CLTVDVLVKIQRDQIQEEALHQVNGLIDSLVVGLRNDPAGTRQRCASFMNACTSQN.VGN 145
Tc   103 CLTVEVKILTQRDKMQEEALHQVNHLIDSLVMCVKSDPESAKARCITFMNACSSNVVHGI 162
```

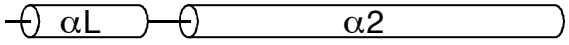


```
dimer    d  dd  d  ddd  d   d  dd  d  dd  d  dd
Hsc70    hhhh hhh hh hh  hh  h
peptide    11 111 112 bb22bb22b  222222  2222
Mm   151 VDQKFQSIVIGCALEDQKKIKRRLETLLRNIDNSDKAIKLLEHAKGAGSKSLQNTDGKFN. 210
Hs   151 VDQKFQSIVIGCALEDQKKIKRRLETLLRNIENSDKAIKLLEHSKGAGSKTLQQNAESRFN 211
Bt   151 VDQKFQSIVIGCALEDQKKIKRRLETLLRNIENADKAIKLLEHSKGAASKTLQQNAEARFN 211
Md   151 IDQKFQSIVIGCALEDQKKIKRRLETLLRNIENSDKAIKLLEHSKGAGSKGLKQTSLNQV. 210
Oa   151 IDQKFQSIVIGCALEDQKKIKRRLETLLRNIDNSDKAIKLLEHSKGAIQKLCNKPE..... 206
Gg   168 IDQKFQSVVIGCAIEDQKKIKRRLETLLRNLENSEKSITLLEHQKSSMRQSCNTKQD.... 224
Xt   156 VDQKFQSIIIGCAIEDQKRIKRRLETLIRNIDNSEKSITLLEQQRQKSAFSLIHTKNL... 213
Br   154 VDQKFQSVVISCALEDQKKIKRRLETLIRNMDNAEKTIQIMDNPKVDLSKLANGK...... 208
Ce   412 TCQNFLKIIIQCAADDQKRIKRRLENLMSQIENAERTKADLMDDQSE.............. 458
Spu  167 VDDRFQGALLGCAAEDQKMIRKKLQEIKESLSETDAFMARLQALKLDL.............. 214
Dm   225 VDKKFESVLLGCTLDDQKNIKKRLQALMAYLNKQTVSH....................... 262
Am   146 SDKNFETAILGCTMDDQKRIKKRLQGLLDYIDKMHTIQLL...................... 185
Tc   168 TDKKFESALLGCTVDDQKRVKKRLQGLLNYFDKLNVTSIP..................... 202
```

Supplementary Figure 1 Sequence alignment of Bag2-BNB domains from different organisms. The corresponding secondary structure elements of the Murine Bag2-BNB domain are shown above the alignments. Residues that participate in BNB domain dimerization are marked above the alignments with "d". Residues that make up the Hsc70 contact interface are marked with "h". Residues that comprise the respective peptide binding sites are marked with "1" (interacts with $CFTR_{481–487}$), "2" (interact with $CFTR_{511–525}$), or "b" (interact with both peptides). The sequences shown are as follows; Mm: murine, *Mus musculus* Bag2); Hs: human, *Homo sapiens* Bag2 ; Bt: bovine, *Bos Taurus* Bag2 ; Md: Opossum, *Monodelphis domestica* ; Oa: Platypus, *Ornithorhynchus anatinus*; Gg: Chicken, *Gallus gallus*; Xt: clawed frog, *Xenopus tropicalis*; Br: zebrafish, *Brachydanio rerio*; Ce: nematode, *Caenorhabditis elegans* Unc-23/NP505307; Spu: sea urchin, *Strongylocentrus purpuratus* XP795015; DM: fruit fly, *Drosophila melanogaster* NP730051; Am: honeybee, *Apis mellifera* XP623942; Tc: red flour beetle, *Tribolium castanea* XP974403.

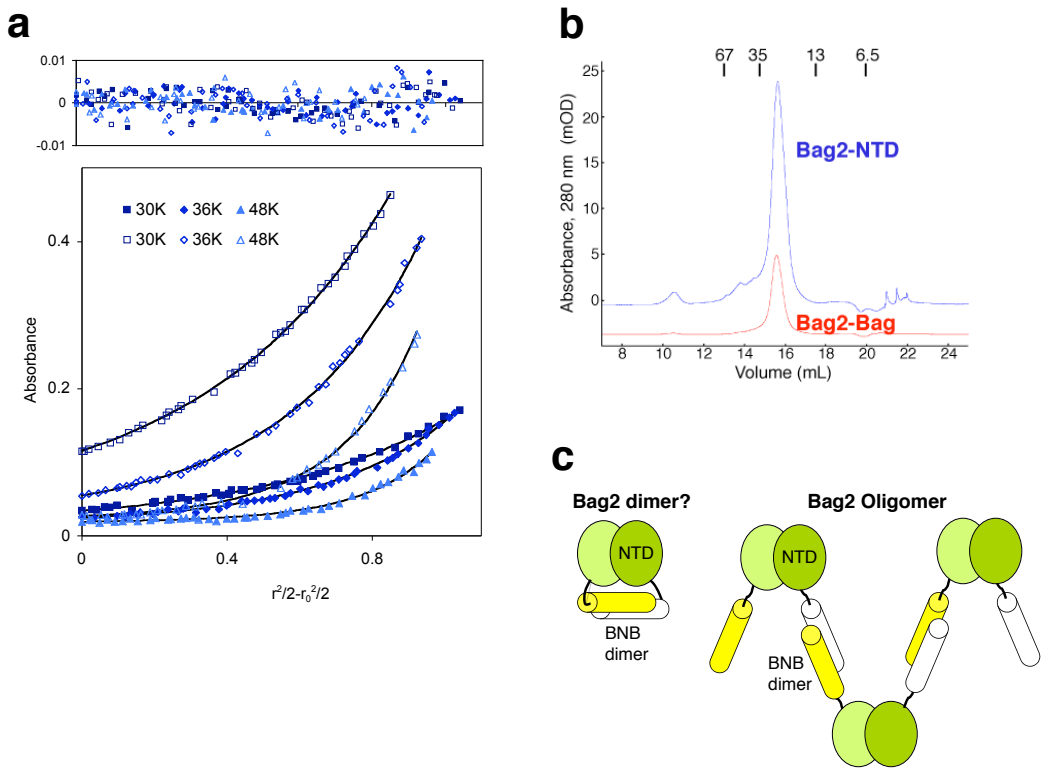

Supplementary Figure 2 Solution measurements of the oligomerization states of Bag2-BNB and Bag2-NTD. (**a**) Representative sedimentation equilibrium data for Bag2-BNB taken from a global fit of three concentrations at speeds of 30K, 36K, and 48K (72,600, 105,000, and 186,000 *g* respectively). Data collected at 235 nm (open symbols) and 280 nm are shown here (closed symbols) with the global fits (black lines) superimposed. Residuals are plotted above the data. These data are best described by a monomer-dimer equilibrium with a K_D of 4.5 μM (95% confidence interval 2.5-6.7 μM). (**b**) Analytical gel filtration of Bag2-NTD and Bag2-BNB using a Superdex-75 column. Both species elute as dimers (monomer moleculer weights of 9.4 and 9.7 kD, respectively). The elution volumes of molecular weight standards are indicated. (**c**) Schematic models of Bag2 dimerization and oligomerization (as observed in sedimentation velocity experiments) through formation of homotypic NTD:NTD and BNB:BNB contacts. The NTD likely dimerizes with higher affinity, while subsequent reversible oligomerization may be mediated by BNB:BNB contacts.

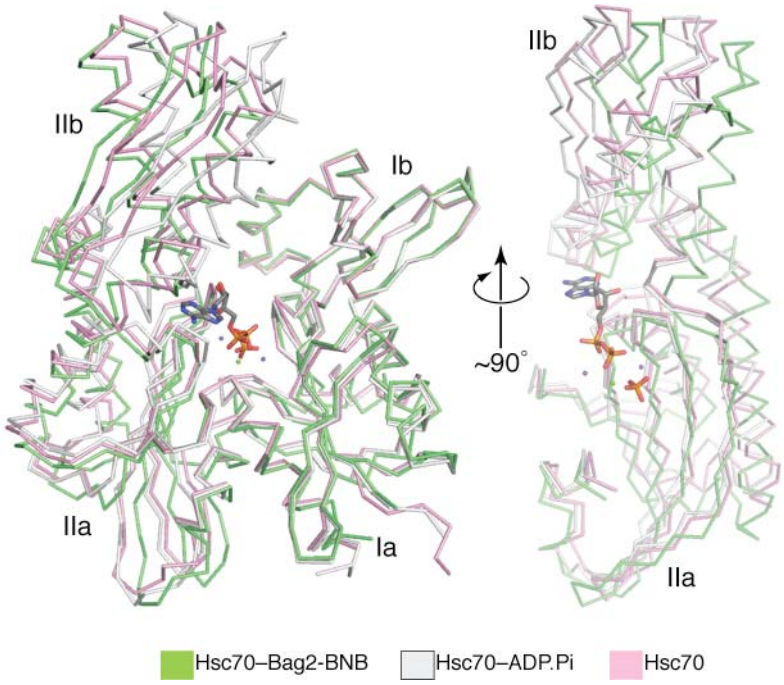

Supplementary Figure 3 Structural comparison between the nucleotide-free and Bag2-BNB-bound Hsc70-NBD. Superimposed structures of the Hsc70-NBD in the Bag2-BNB-bound form (green), ADP·Pi-bound form (grey; PDB code 3HSC) and nucleotide-free form (pink; PDB code 1YUW). The bound nucleotide in the ADP·Pi complex is shown in stick representation. In the right panel, Hsc70-NBD domain I has been removed and the view is looking at the nucleotide binding site on domain II. Structures are aligned based on domain I, emphasizing changes in the orientations of subdomains IIa and IIb relative to domain I. The Rmsd values in the orientations shown are 3.1 Å (BNB-bound vs. ADP-Pi-bound form) and 2.4 Å (BNB-bound vs. nucleotide-free form) respectively. For comparison, the Rmsd for the BNB-bound vs. the Bag1-bound form of the Hsc70-NBD in the equivalent superimposition is 2.4 Å. The structures emphasize that Bag2-BNB binding induces conformational changes in the Hsc70-NBD that are distinct from those observed in the nucleotide-free form. This suggests that the changes are not merely due to the dissociation of nucleotide upon Bag2-BNB binding.

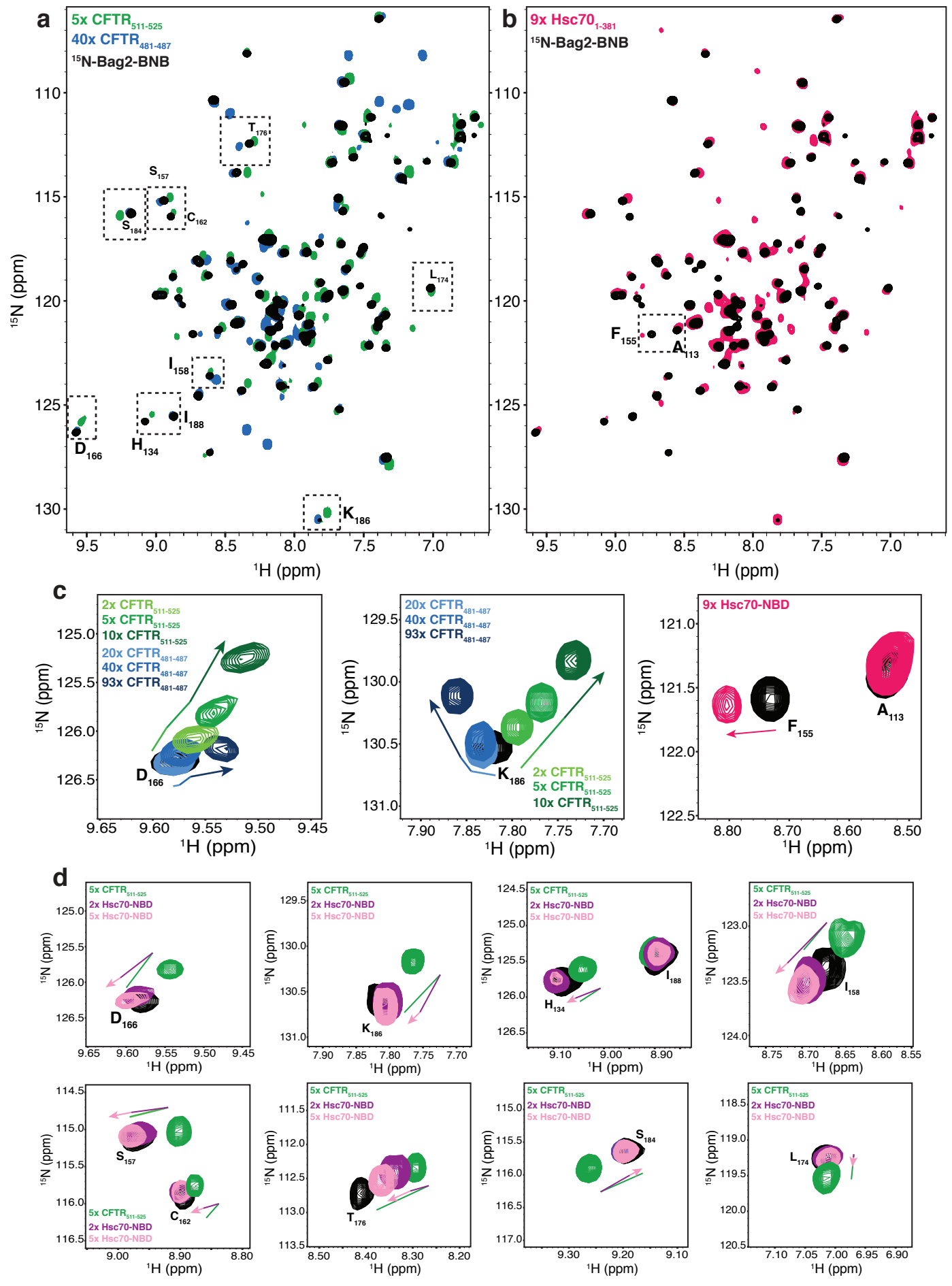
a
5x CFTR511-525
40x CFTR481-487
15N-Bag2-BNB
T176
S157
S184
C162
L174
I158
I188
H134
D166
K186
15N (ppm)
1H (ppm)
b
9x Hsc701-381
15N-Bag2-BNB
F155
A113
15N (ppm)
1H (ppm)
c
2x CFTR511-525
5x CFTR511-525
10x CFTR511-525
20x CFTR481-487
40x CFTR481-487
93x CFTR481-487
D166
15N (ppm)
1H (ppm)
20x CFTR481-487
40x CFTR481-487
93x CFTR481-487
K186
2x CFTR511-525
5x CFTR511-525
10x CFTR511-525
15N (ppm)
1H (ppm)
9x Hsc70-NBD
F155
A113
15N (ppm)
1H (ppm)
d
5x CFTR511-525
2x Hsc70-NBD
5x Hsc70-NBD
D166
K186
H134
I188
I158
S157
C162
T176
S184
L174
15N (ppm)
1H (ppm)

Supplemental Figure 4 HSQC titrations of Bag2-BNB domain. $^{1}H/^{15}N$-HSQC spectra for Bag2-BNB demonstrate binding with CFTR-derived peptides and Hsc70-NBD. Additional spectra collected at different ratios of peptides and Hsc70-NBD to Bag2-BNB were collected but are not shown. Peak labels are based on assignment of the free forms of the Bag2-BNB. Assignments of the complexed forms were deduced by comparison with the free form. Peaks shown as close-ups in (**c**) and (**d**) are labeled and marked in dashed boxes. (**a**) Superimpositions of ^{15}N-Bag2-BNB (black) with 40:1 $CFTR_{481–487}$:Bag2-BNB (blue) and 5:1 $CFTR_{511–525}$:Bag2-BNB (green). (**b**) Superimpositions of ^{15}N-Bag2-BNB (black) with 9:1 Hsc70-NBD:Bag2-BNB (pink). (**c**) Selected peaks from $^{1}H/^{15}N$ HSQC titrations, colored as in (**a**) and (**b**). The unperturbed peaks from free ^{15}N-Bag2-BNB are shown in black. (**d**) Selected peaks from a competition titration experiment. Spectra were collected from free ^{15}N-Bag2-BNB (black) and the same sample with 5:1 unlabeled $CFTR_{511-525}$ (green). Subsequently, the Bag2-BNB:$CFTR_{511–525}$ complex was titrated with increasing amounts of unlabeled Hsc70-NBD (purple, pink). Upon addition of Hsc70-NBD, ^{15}N-Bag2-BNB peaks are perturbed to positions characteristic of the Hsc70-NBD:Bag2-BNB complex, suggesting that Hsc70-NBD displaces the $CFTR_{511–525}$ peptide from Bag2-BNB. Colored arrows show the directions of chemical shift perturbations from free Bag2-BNB to the Bag2-BNB:$CFTR_{511–525}$ complex (green) and back to the Hsc70-NBD:Bag2-BNB complex (purple/pink).

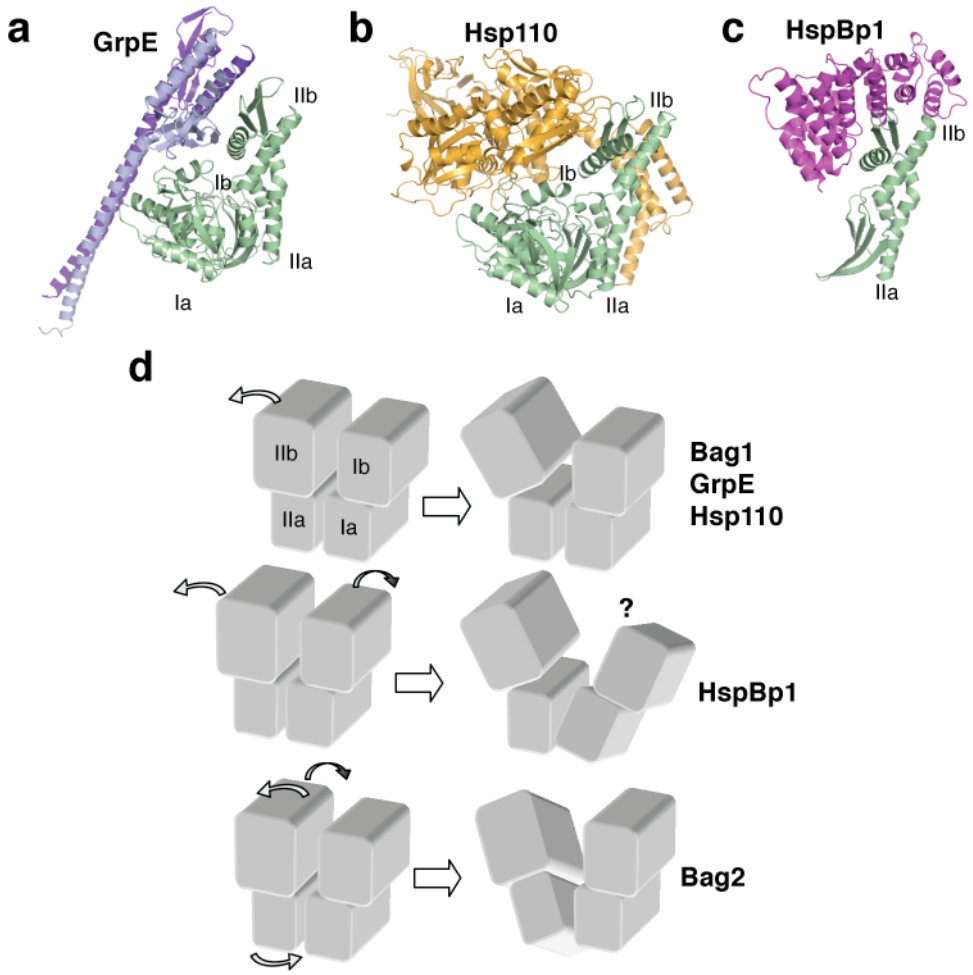

Supplementary Figure 5 Comparison of binding modes and conformational changes caused by different Hsp70 nucleotide exchange factors. The structures in panels (**a**)-(**c**) are shown in an orientation rotated ~170˚ about the y axis and tilted ~60˚ about the x axis from the views in **Fig. 3a,b**. (**a**) *E. coli* GrpE dimer bound to the NBD of the bacterial Hsp70 chaperone DnaK (PDB ID: 1DKG). (**b**) Hsp110 complexed with Hsp70-NBD (PDB ID: 3D2F). (**c**) Ankyrin-repeat-like domain from HspBP1 complexed with domain II of the Hsp70-NBD (PDB ID: 1XQS). HspBP1 could not be crystallized with the entire Hsp70-NBD, possibly due to an extensive clash with and dislocation of NBD domain I. (**d**) Schematic representation of the conformational changes in the NBD caused by binding of different Hsp70-NEFs. Each block represents a subdomain of the NBD, as marked in the top scheme. Small arrows indicate domain or subdomain rotations induced by the respective NEFs. The conformational change for HspBp1 is modeled after a similar depiction by Shomura and coworkers. (Shomura, Y. *et al*. Regulation of Hsp70 function by HspBP1: structural analysis reveals an alternate mechanism for Hsp70 nucleotide exchange. *Mol. Cell* **17**, 367-79 (2005)).

Sedimentation velocity analyses of Bag2 constructs

	Frictional coefficient f/f_0	Sedimentation coefficient (Svedbergs)	Estimated MW (kDa)	Monomer MW from sequence (kDa)
Bag2	1.12	1.93 ± 0.28	~15	21.7
		4.35 ± 0.84	~88	
		8.70 ± 2.37	~180	
		19.8 ± 0.2	~510	
Bag2-BNB	1.53	1.64 ± 0.30	~19	9.69

Supplementary Table 1 Results of sedimentation velocity measurements on near-full-length murine Bag2 and Bag2-BNB domain. Bag2-BNB is primarily present as a dimer, while full-length Bag2 is primarily tetrameric with additional higher-order oligomers. The identity of the low-molecular weight (15 kD) component of the Bag2 sedimentation profile is unclear and may represent a degradation product.

SUPPLEMENTARY METHODS

Expression and purification of constructs for *in vitro* assays. A GST-fused full, near-full length human Bag2 construct, pGEX-6p-1-Hs.Bag2$_{4-211}$ has been described previously (Ref. 10). Site-directed mutations were introduced into this construct using the Quikchange mutagenesis kit (Stratagene) and verified by sequencing. Wild-type and mutant GST-HsBag2 fusion proteins were expressed in Rosetta2(DE3) cells and purified by a protein miniprep procedure using the GST SpinTrap Purification Module (GE Healthcare). These proteins were used for GST pulldown (minicolumn binding) experiments and single-turnover nucleotide exchange assays.

Murine Bag2 (MmBag2$_{21–210}$) containing both the NTD and BNB domains, was cloned into the pGSTII2 vector as a GST-fusion protein. HsBag2 (above) and MmBag2 were expressed in Rosetta2(DE3) cells and purified by glutathione-affinity chromatography using a GSTPrep FF column (GE Healthcare). GST tags were removed by overnight cleavage with Thrombin (HsBag2) or TEV protease (MmBag2), followed by a second pass over the GSTPrep FF column. These untagged proteins were used for analytical ultracentrifugation and Luciferase refolding assays.

The N-terminal domain of murine Bag2 (Bag2$_{21–90}$) and human Hsp40 were cloned into the pHisII2 vector and expressed as His-tagged fusion proteins in Rosetta2(DE3) cells. Proteins were purified by Nickel affinity chromatography using a similar procedure as that described for the Bag2-BNB. The Bag2-NTD was used for gel filtration, while Hsp40 was used in Luciferase refolding assays.

GST-pulldown (minicolumn binding) assays. For GST-pulldown assays, 30 μg of GST-tagged human Bag2 proteins or Glutathione S-transferase (GST) in 100 μl PBS buffer were immobilized on pre-equilibrated GST-spin columns (GE Healthcare) during overnight incubations at 4 °C. Minicolumns were washed 3 times and incubated with purified Hsc70-NBD for 3.5 hours at 4 °C, followed by 4 washes with 500 μl PBS each. Bound proteins were eluted with 10 mM glutathione in 100 μl PBS. The final wash and elution were subjected to SDS-PAGE and Coomassie blue staining.

Analytical ultracentrifugation experiments. Sedimentation velocity and equilibrium experiments were carried out in a Beckman XL-I ProteomeLab analytical ultracentrifuge with absorbance optics. Samples were prepared in 50 mM Tris, 150mM NaCl at pH 7.4. In the sedimentation velocity experiments, 410 μl of Hsc70-NBD, murine Bag2 21-210, or Bag2-BNB were loaded into two-sector charcoal-filled epon centerpieces and spun at 48,000 rpm [c1]at 20 °C. Data were analyzed using c(s) and c(M) models in SEDFIT[1]. Sedimentation equilibrium experiments on Bag2-BNB were carried out at 20 °C at 72,600, 105,000, and 186,000 *g* (30,000, 36,000 and 48,000 rpm respectively). 100 μl samples at concentrations between 9.6 and 87 μM were loaded into six-channel centerpieces. Radial scans at 230, 235 and 280nm were collected as the average of eight scans. Data was trimmed using WinREEDIT and globally fitted using WinNONLIN (http://www.rasmb.bbri.org/) to a single exponential to determine σ_w, the weight-average buoyant molecular weight, which corresponded approximately to a dimer. A monomer-dimer assembly model was used to analyze the data[2]. Higher-order assembly models did not result in improvement in the fit. The partial specific volume of Bag2-BNB was calculated based on amino acid sequence to be 0.739 ml g^{-1} and buffer density was calculated as 1.01 g ml^{-1} using SEDNTERP[3]. Calculation of experimental molecular weights from σ and conversion of the

monomer-dimer equilibrium constant from absorbance units into molar units were performed as described[2,4].

Nucleotide exchange assays. Hsc70 (1 mM) was incubated with equimolar amounts of wild-type or mutant human GST-Bag2 in 20 mM HEPES, 10 mM $(NH_4)_2SO_4$, 25 mM KCl, 2 mM $Mg(C_2H_3O_2)_2$, 0.1 mM EDTA, 0.1 mM DTT. 1 μCi of α-^{32}P-ATP was added to the incubation. After ATP hydrolysis, radioactive ADP binding to Hsc70 was quantitated by thin layer chromatography on Selecto Cellulose polyethyleneimine sheets using 1 M formic acid and 1 M LiCl. Unlabeled ATP and ADP were used as standards. Sheets were dried and exposed to film, and nucleotide binding was quantified by densitometry.

Luciferase refolding assays. To measure the time dependence of Luciferase refolding, 1 μM recombinant Hsc70 (Stressgen), 1 μM Hsp40 and 1 μM Bag2 constructs were preincubated in 25 mM HEPES pH 7.6, 50 mM KCl, 5 mM $MgCl_2$ with 5 mM DTT and 2 mM ATP for 5 min at 20˚C. Firefly luciferase (Sigma-Aldrich) was added to 0.1 μM and the reactions were heated at 42˚C for 20 min to denature the luciferase. The refolding reaction (20 μl) was initiated by addition of 5% rabbit reticulocyte lysate with hemin (Promega) and 2.5 mM ATP and incubation at 30˚C. At selected time points, 1 μl aliquots from the refolding reactions were diluted into 10 μl of assay buffer and analyzed for bioluminescence activity using a Veritas microplate luminometer (Turner Biosystems) after addition of 100 μl of Luciferase assay reagent (Promega). The enzymatic activity of non-denatured luciferase incubated at 30˚C in refolding buffer containing Hsc70 and Hsp40 was set to 100%. The concentration dependendence of luciferase refolding was assayed in a similar manner, except that the concentration of the Bag2 constructs were varied and Luciferase activity was measured at 60 min. Addition of BSA was used as a negative control.

REFERENCES for Methods

1. Schuck, P. Size-distribution analysis of macromolecules by sedimentation velocity ultracentrifugation and lamm equation modeling. *Biophys. .J.* **78**, 1606-19 (2000).

2. Herr, A.B., Ornitz, D.M., Sasisekharan, R., Venkataraman, G. & Waksman, G. Heparin-induced self-association of fibroblast growth factor-2. Evidence for two oligomerization processes. *J. Biol. Chem.* **272**, 16382-9 (1997).

3. Laue, T.M., Shah, B.D., Ridgeway, T.M. & Pelletier, S.L. Computer-aided interpretation of analytical sedimentation data for proteins. in *Analytical ultracentrifugation in biochemistry and polymer science* (eds. Harding, S.E., Rowe, A.J. & Horton, J.C.) 90-125 (The Royal Society of Chemistry, Cambridge, U.K., 1992).

4. Herr, A.B., White, C.L., Milburn, C., Wu, C. & Bjorkman, P.J. Bivalent binding of IgA1 to FcalphaRI suggests a mechanism for cytokine activation of IgA phagocytosis. *J .Mol. Biol.* **327**, 645-57 (2003).